

Received 26 November 2016; accepted 10 January 2017. Date of current version 22 February 2017. The review of this paper was arranged by Editor C. Surya.

Digital Object Identifier 10.1109/JEDS.2017.2653419

# Characterizations of Metal-Oxide-Semiconductor Field-Effect Transistors of ZnGaO Grown on Sapphire Substrate

YI-SIANG SHEN<sup>1</sup>, WEI-KAI WANG<sup>2</sup>, AND RAY-HUA HORNG<sup>1,3</sup> (Fellow, IEEE)

<sup>1</sup> Graduate Institute of Precision Engineering, National Chung Hsing University, Taichung 402, Taiwan

<sup>2</sup> Department of Materials Science and Engineering, Da-Yeh University, Changhua 515, Taiwan

<sup>3</sup> Institute of Electronics, National Chiao Tung University, Hsinchu 300, Taiwan

CORRESPONDING AUTHOR: R.-H. HORNG (e-mail: rhh@nctu.edu.tw)

This work was supported by the Ministry of Science and Technology, Taiwan, under Contract MOST104-2221-E-009-199-MY3.

**ABSTRACT** Zinc gallate (ZnGaO) epilayers were grown on a c-plane sapphire substrate by metalorganic chemical vapor deposition and fabricated into metal-oxide-semiconductor field-effect transistors (MOSFETs). The ZnGaO MOSFETs exhibited a complete channel pinch-off of the drain current for  $V_{GS} < -4.43$  V, high off-state breakdown voltage of 378 V, high  $I_{ON}/I_{OFF}$  ratio of  $10^6$ , and low gate leakage current.

**INDEX TERMS** Zinc gallate, metal-oxide-semiconductor field-effect transistors (MOSFETs), channel pinch-off.

## I. INTRODUCTION

Wide-band gap oxides have attracted interests as new materials and possess unique properties for application in next-generation semiconductor power devices and deep ultra-violet (UV) detectors [1], [2]. Among these oxides, ZnGa<sub>2</sub>O<sub>4</sub> has been paid great attention as a transparent conducting oxide in the UV region due to its high chemical stability and outstanding optical properties [3]–[5]. The material ZnGa<sub>2</sub>O<sub>4</sub> consists of ZnO and Ga<sub>2</sub>O<sub>3</sub>, which crystallizes in the spinel structure and has an energy gap of about 5.2 eV [6]. In previous report, ZnGa<sub>2</sub>O<sub>4</sub> is a phosphor and is a promising application in field emission displays operating at low accelerating voltage [7]. Up to now, most of the reports are relative to the synthesis of ZnGa<sub>2</sub>O<sub>4</sub> nanostructures with different morphologies, such as nanowires, nanorods and nanocrystal [8]–[10]. The corresponding electronic transport and optical properties of the ZnGa<sub>2</sub>O<sub>4</sub> nanostructure were also studied [11]. However, there are still very few works to investigate the film and epilayer properties of ZnGa<sub>2</sub>O<sub>4</sub>. In addition, as far as we know, no relevant research about MOSFET based on ZnGa<sub>2</sub>O<sub>4</sub> epilayer has been reported yet. In this work, the material qualities of zinc gallate (ZnGaO; ZGO) were described. Moreover, MOSFETs made of ZGO epilayers

grown on c-plane sapphire by MOCVD were also studied. The device performances indicated that the ZGO MOSFET has potential for application in transparent power electronic devices.

## II. DEVICE STRUCTURE AND FABRICATION

ZGO MOSFETs were fabricated using 200-nm-thick single-crystal ZGO epilayers grown on c-plane (0001) sapphire substrates at 600°C by metalorganic chemical vapor deposition. Diethylzinc (DEZn) and triethylgallium (TEGa) were employed as the Zn and Ga precursors, respectively. Ar (99.999 %) and purified oxygen (99.999 %) were adopted as carrier gases and oxidizer, respectively. During the growth of ZGO thin films, Ar passed through the bubblers to deliver the DEZn and TEGa vapors to the reactor. After growth, the intrinsic ZGO is a n-type epilayer confirmed by Hall measurement. In order to demonstrate the film was ternary epilayer, the x-ray diffractometry was used to measure the crystal structure. The electrical mobility, resistivity, and electron concentration of ZGO used for the MOSFET study were 2.2 cm<sup>2</sup>/V.s, 47.5 Ω.cm, and  $5.9 \times 10^{16}$  cm<sup>-3</sup>, respectively, and were obtained through Hall measurement at room temperature (RT). The process commenced with mesa isolation

in an inductively coupled plasma reactive ion etching system by using  $\text{BCl}_3/\text{Cl}_2/\text{Ar}$ . Ti/Al/Ti/Au (25/125/50/60 nm) was evaporated to form the metal contacts for the source (S) and drain (D) electrodes. Notably, the Ti metal contacting to ZGO exhibited ohmic contact behavior without any thermal annealing. The 40-nm  $\text{Al}_2\text{O}_3$  dielectric layer was deposited through ALD at  $300^\circ\text{C}$ . Finally, Ni/Au (150/50 nm) gate metals were deposited on the  $\text{Al}_2\text{O}_3$  by e-beam evaporation. The lengths of the device channel, gate, and the access region were  $20\ \mu\text{m}$ ,  $L_G = 3\ \mu\text{m}$ , and  $L_{GS} = L_{GD} = 8.5\ \mu\text{m}$ , respectively. The current-voltage ( $I$ - $V$ ) characteristics of these samples were measured using an Agilent 1505B parameter analyzer at RT. In order to evaluate the crystal structure of the ZGO epilayer, the X-ray diffraction (XRD, PANalytical, Cu  $K\alpha$  radiation) was used to measure the crystalline quality. Microstructure of the ZGO film was investigated by transmission electron microscopy (TEM).

### III. RESULTS AND DISCUSSION

Fig. 1 shows the XRD diffraction pattern of ZGO film grown on sapphire substrate. The XRD pattern shows strong peak at around  $42^\circ$  which was identified to be the  $\text{Al}_2\text{O}_3$  (0006) plane. Moreover, the monoclinic  $\beta$ - $\text{Ga}_2\text{O}_3$  film with very small peak located at diffraction angles of  $38.4^\circ$  corresponding to the (-402) planes reflections was obtained. It was also found that there were additional features of diffraction intense peaks observed at  $18.57^\circ$ ,  $37.61^\circ$ , and  $57.82^\circ$ . These peaks very closed to the  $18.40^\circ$ ,  $37.34^\circ$ , and  $57.40^\circ$  characteristic reflections of (111), (222) and (333) crystal planes of  $\text{ZnGa}_2\text{O}_4$  (JCPDS card 381240). These results indicated that the epilayer has transferred most of  $\text{Ga}_2\text{O}_3$  into the ZGO epilayer. The measured XRD data are also shown in Table 1.

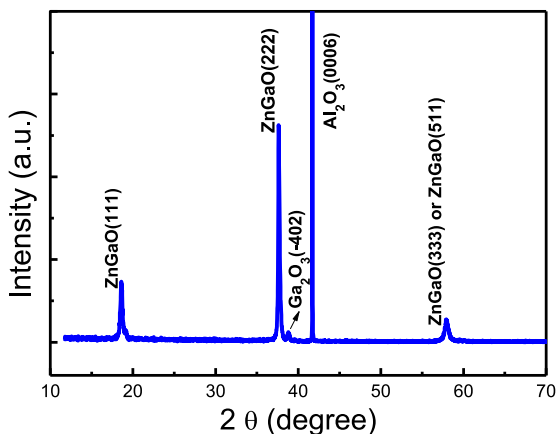


**FIGURE 1.** XRD pattern of ZGO film grown on c-plane sapphire substrate.

Fig. 2(a) shows the high-resolution TEM bright field image focused on the interface between ZGO film and c-plane sapphire substrate. According to our analysis, the d-spacing of  $2.42\ \text{Å}$  of ZGO film was obtained in this image, which was very close to the standard d-spacing of  $2.406\ \text{Å}$  of  $\text{ZnGa}_2\text{O}_4$ (222) plane. In addition, the high-resolution TEM bright field image taken at the middle region of ZGO film

**TABLE 1.** XRD diffraction measured results of ZGO film.

$\text{ZnGa}_2\text{O}_4$ (Cubic, fcc)	$\text{Ga}_2\text{O}_3$ (Monoclinic)	ZnO (Hexagonal)	ZGO (Epilayer)
$18.40^\circ$ (111)	$18.95^\circ$ (-201)		$18.57^\circ$ (111)
$37.34^\circ$ (222)	$38.39^\circ$ (-402)	$36.25^\circ$ (101)	$37.61^\circ$ (222)
$57.40^\circ$ (511)	$59.19^\circ$ (-603)	$56.25^\circ$ (101)	$57.82^\circ$ (333)

is displayed in Fig. 2(b). Based on our observation, the most lattice features shown in Fig. 2(b) belonged to that marked with green parallel lines. These lattices possess the d-spacing value of  $4.809\ \text{Å}$ , where the standard d-spacing of  $\text{ZnGa}_2\text{O}_4$ (111) plane is  $4.808\ \text{Å}$ . On the other hand, a fraction of lattice features presented in this image was also labeled with yellow parallel lines, and its d-spacing was much similar to the standard one of  $\text{Ga}_2\text{O}_3$ (-402) plane. Obviously, the TEM observations are in well agreement with the XRD result, as shown in Fig. 1. In other words, the main crystal structure formed in the ZGO film is the  $\text{ZnGa}_2\text{O}_4$  phase with the (111)-family planes. Besides, a small portion of  $\text{Ga}_2\text{O}_3$ (-402) phase existed in the ZGO film also can be confirmed by TEM. Fig. 2(c) shows the selected area electron diffraction pattern of the  $\text{ZnGa}_2\text{O}_4$  region shown in Fig. 2(b). The diffraction dots with a regular arrangement indicates the microstructure is single crystalline. Moreover, this single crystalline diffraction pattern reveals the  $\text{ZnGa}_2\text{O}_4$  phase of ZGO film is formed along the [111] direction (with the [1-21] zone axis).

In order to demonstrate the epilayer has become the ZGO film, the energy gap of ZGO was evaluated by cathodeluminescence (CL) measurement. Fig. 3 shows CL spectrum of ZGO film at RT. The spectrum consists of two ultraviolet (UV) luminescence emission bands at the wavelength peaks position of  $330\ \text{nm}$  ( $3.75\ \text{eV}$ ;  $E_{\text{CL}1}$ ) and  $242\ \text{nm}$  ( $5.12\ \text{eV}$ ), respectively. In the visible region, there exists a weak intensity at peak of  $500\ \text{nm}$  ( $2.48\ \text{eV}$ ;  $E_{\text{CL}2}$ ). The weaker CL intensity at peak  $242\ \text{nm}$  could be due to the conduction band to the valence band transition of ZGO. Theoretically, the  $E_g$  of  $\text{ZnGa}_2\text{O}_4$  is about  $5.2\ \text{eV}$ . In this work, the ZGO is not a perfect  $\text{ZnGa}_2\text{O}_4$ . Nevertheless, it has demonstrated again that the epilayer is the ZGO and not Zn-dopant  $\text{Ga}_2\text{O}_3$ . On the other hand, a strong UV emission band ( $330\ \text{nm}$ ) could be attributed to the radiative carriers transition from the donor level ( $E_d$ ) to the valence band. Although the ZGO is the dominated structure, there exists a few part of  $\beta$ - $\text{Ga}_2\text{O}_3$  (demonstrated by XRD and TEM, shown in Figs. 1 and 2). Obviously, suppress of intrinsic green emission band centered at around  $500\ \text{nm}$  which is induced by donor-acceptor-pair transition in  $\beta$ - $\text{Ga}_2\text{O}_3$  through Zn-incorporation, and further contribution on the UV emission band was obtained. Based on above analysis, the  $E_d$  was estimated to be approximately about  $1.37\ \text{eV}$  by a formula  $E_d = E_g - E_{\text{CL}1}$ , which is consists with previous reported by Varley *et al.* [12]. An acceptor level ( $E_a$ ) for the  $\text{Zn}_{\text{Ga}}$  was calculated to be  $1.27\ \text{eV}$ ,

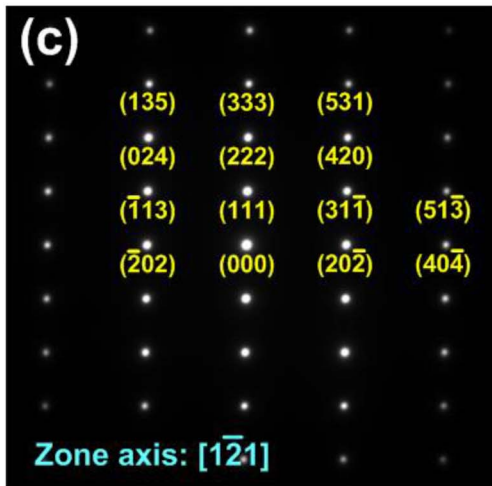
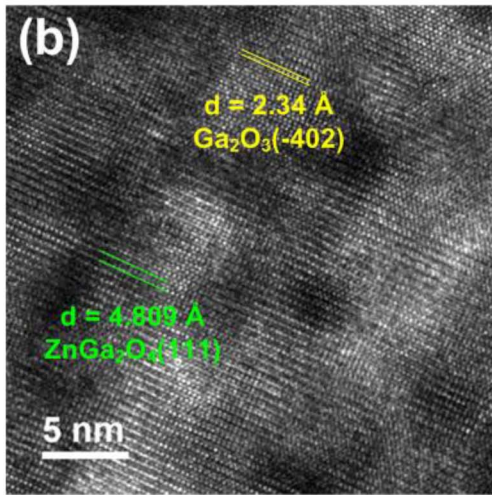
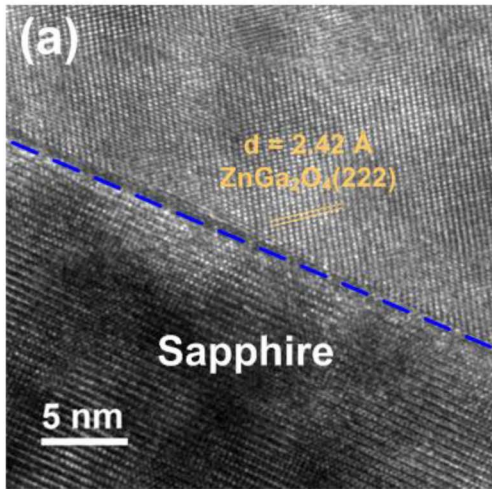


**FIGURE 2.** HR-TEM images taken at (a) the interface between ZGO and sapphire and (b) the middle region of ZGO film. (c) Selected area electron diffraction pattern of  $ZnGa_2O_4$  phase shown in Fig. 2(b).

( $E_a = E_{CL1} - E_{CL2}$ ). Schematic diagram of the energy levels in the ZGO film is also illustration in the inset of Fig. 3.

Fig. 4 shows the DC output I-V ( $I_{DS}$ - $V_{DS}$ ) characteristics of ZGO MOSFET at gate voltage ( $V_{GS}$ ) from -5 to 15 V

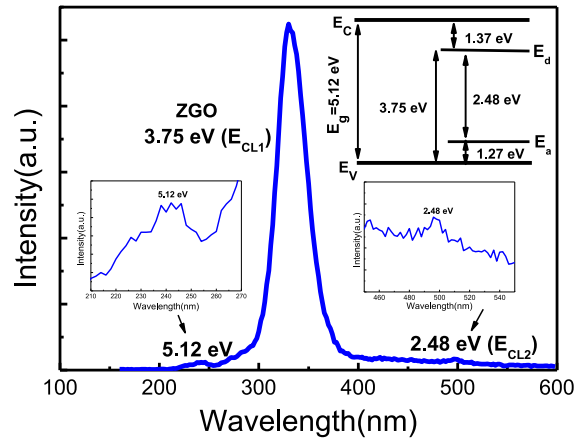


**FIGURE 3.** CL spectrum of ZGO film grown on sapphire substrate measured at RT. Insets are the magnified 5.12 eV, 2.48 eV spectra and the energy levels diagram in the ZGO film.

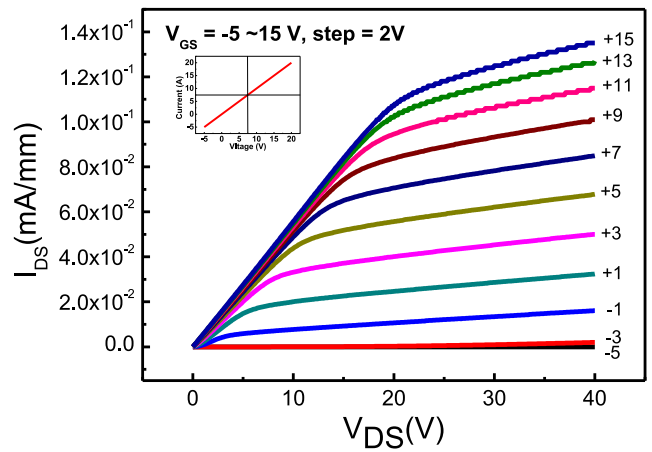


**FIGURE 4.** DC I-V characteristics of ZGO MOSFET measured at RT.

in steps of 2 V, while the  $V_{DS}$  was swept from 0 to 40 V at RT. The device exhibited a clear pinch-off behavior and maximum  $I_{DS}$  of 0.135 mA/mm at  $V_{GS} = +15$  V. In addition, the transistor shows favorable gate-modulation performance with  $I_d$  saturation, whereas the channel mobility and sub-threshold slope of ZGO MOSFET were calculated about  $2.46 \text{ cm}^2/\text{V}\cdot\text{s}$  and  $40 \text{ mV}/\text{decade}$ , respectively. Moreover, the insert plot in Fig. 4 shows the linear I-V characteristic of Ti/Al/Ti/Au on ZGO without thermal annealing. Obtaining ohmic contacts was thus easy in this study because Ti metal layer can be ohmic contact with the ZGO. Similar reports on the ohmic contact through Ti/Al/Ti/Au multiple metals were found by Wang *et al.* [13].

Fig. 5 shows the transfer characteristics at a  $V_{DS}$  of 13 V. The threshold voltage on ZGO MOSFET was  $-4.43$  V, which suggests that the device presented the depletion mode characteristic. Clearly, the ZGO was n-type and could enhance the conductivity through formation oxygen vacancy due to Zn atom compensation effect [14]. However, it is necessary to attract more electrons by applying

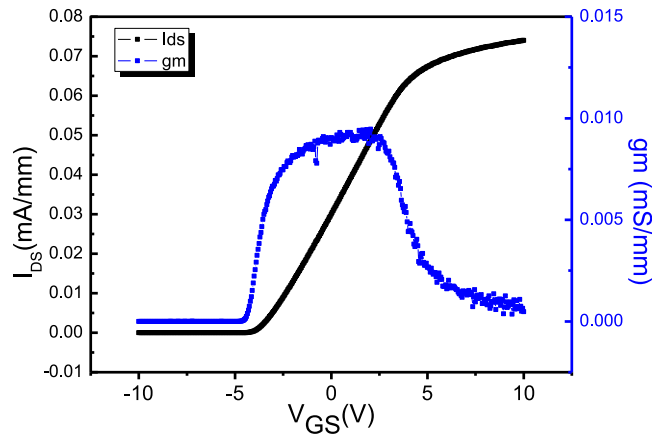


**FIGURE 5.** Transfer characteristics of ZGO MOSFET at  $V_{DS}=13$  V measured at RT.

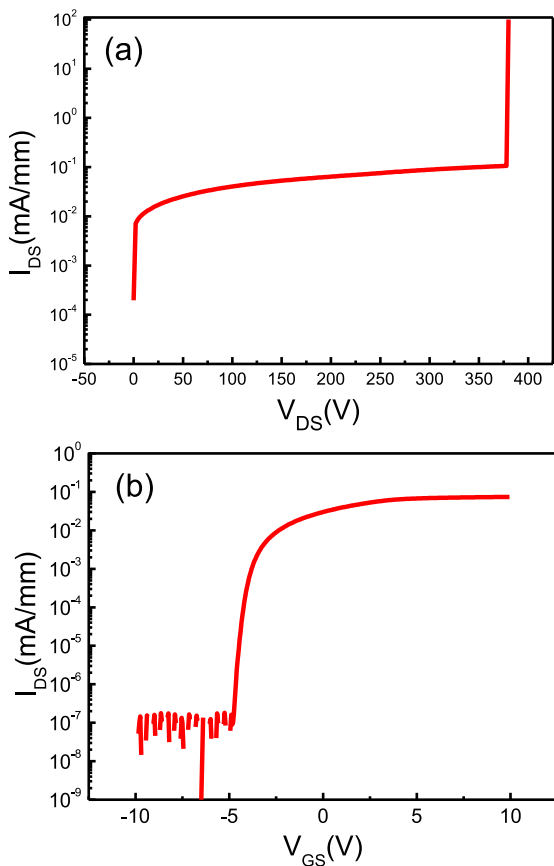


**FIGURE 6.** (a) Breakdown voltage characteristic of ZGO MOSFET and (b)  $I_{DS}$ - $V_{GS}$  curve of ZGO MOSFET measured at 13 V of  $V_{DS}$ .

positive voltage on gate electrode to switch the transistor on. The peak intrinsic maximum transconductance ( $g_m$ ) was  $9.46 \times 10^{-3}$  mS/mm at a  $V_{DS}$  of 13 V, which could be attributed to the both of substitutional defects (from Zn-incorporated into  $\beta$ - $\text{Ga}_2\text{O}_3$ ) and the lattice mismatch between the sapphire substrate and ZGO film. These defects resulted in the reduction of electron density and mobility in the ZGO film. Moreover, the carriers' scattering effect,

attributable to defects and impurities, reduced the mobility of the ZGO MOSFET. These results are consistent with those of Dang *et al.* [15].

The three-terminal breakdown behavior of the ZGO MOSFET device was evaluated and is shown in Fig. 6 (a). The breakdown voltage could be attributed to the leakage current through the  $\text{Al}_2\text{O}_3$  layer or ZGO epilayer breakdown. However, a low gate leakage current was less than  $1.45 \times 10^{-5}$  mA/mm (data not shown) from the ZGO film device. Therefore, the breakdown voltage was as high as 378 V at  $V_{GS}$  of 0 V, indicating that ZGO MOSFET with Zn-incorporated exhibits enhanced off-state breakdown voltage. Nevertheless, the measured reverse gate leakage is low enough for device application. Fig. 6 (b) presents the  $I_{DS}$ - $V_{GS}$  curve of ZGO MOSFET at a  $V_{DS}$  of 13 V. The low off-state leakage current ( $10^{-7}$  mA/mm) through the ZGO film was a result of the  $\text{Al}_2\text{O}_3$  gate dielectric. At a  $V_{DS}$  of 13 V,  $I_{DS}$  on/off ratio of approximately six orders of magnitude were achieved.

#### IV. CONCLUSION

We have fabricated ZGO MOSFET on a c-plane sapphire substrate and obtained improved device characteristics, such as a high  $I_{ON}/I_{OFF}$  drain current ratio of six orders of magnitude, clear pinch-off behavior, and breakdown voltage of 378 V. Moreover, we have demonstrated the strong potential of the cost-effective growth of ZGO-on-sapphire for application in future transparent electronic power devices.

#### REFERENCES

- [1] H. He *et al.*, "First-principles study of the structural, electronic, and optical properties of  $\text{Ga}_2\text{O}_3$  in its monoclinic and hexagonal phases," *Phys. Rev. B.*, vol. 74, no. 19, Nov. 2006, Art. no. 195123.
- [2] X. H. Wang *et al.*, "Electrical properties and emission mechanisms of Zn-doped  $\beta$ - $\text{Ga}_2\text{O}_3$  films," *J. Phys. Chem. Solids*, vol. 75, no. 11, pp. 1201–1204, Nov. 2014.
- [3] I. J. Hsieh, K. T. Chu, C. F. Yu, and M. S. Feng, "Cathodoluminescent characteristics of  $\text{ZnGa}_2\text{O}_4$  phosphor grown by radio frequency magnetron sputtering," *J. Appl. Phys.*, vol. 76, no. 6, pp. 3735–3739, Sep. 1994.
- [4] L. E. Shen, R. K. Datta, and J. J. Brown, Jr., "Photoluminescence of  $\text{Mn}^{2+}$ -activated  $\text{ZnGa}_2\text{O}_4$ ," *J. Electrochem. Soc.*, vol. 141, no. 7, pp. 1950–1954, Jul. 1994.
- [5] I. K. Jeong, H. L. Park, and S. I. Moh, "Photoluminescence of  $\text{ZnGa}_2\text{O}_4$  mixed with  $\text{InZnGaO}_4$ ," *Solid State Commun.*, vol. 108, no. 11, pp. 823–826, Mar. 1994.
- [6] T. Omata, N. Ueda, K. Ueda, and H. Kawazoe, "New ultraviolet-transport electroconductive oxide,  $\text{ZnGa}_2\text{O}_4$  spinel," *Appl. Phys. Lett.*, vol. 64, no. 9, pp. 1077–1079, Feb. 1994.
- [7] S. H. Yang, "Electrophoretic prepared  $\text{ZnGa}_2\text{O}_4$  phosphor film for FED," *J. Electrochem. Soc.*, vol. 150, no. 10, pp. H250–H253, Sep. 2003.
- [8] L. Zou, X. Xiang, M. Wei, F. Li, and D. G. Evans, "Single-crystalline  $\text{ZnGa}_2\text{O}_4$  spinel phosphor via a single-source inorganic precursor route," *Inorg. Chem.*, vol. 47, no. 4, pp. 1361–1369, Jan. 2008.
- [9] K.-W. Chang and J.-J. Wu, "Formation of well-aligned  $\text{ZnGa}_2\text{O}_4$  nanowires from  $\text{Ga}_2\text{O}_3/\text{ZnO}$  core-shell nanowires via a  $\text{Ga}_2\text{O}_3/\text{ZnGa}_2\text{O}_4$  epitaxial relationship," *J. Phys. Chem. B.*, vol. 109, no. 28, pp. 13572–13577, Jan. 2005.
- [10] M.-Y. Lu, X. Zhou, C.-Y. Chiu, S. Crawford, and S. Gradeček, "From GaN to  $\text{ZnGa}_2\text{O}_4$  through a low-temperature process: Nanotube and heterostructure arrays," *Appl. Mater. Interfaces*, vol. 6, no. 2, pp. 882–887, Jan. 2014.



- [11] S. C. Yan *et al.*, "A room-temperature reactive-template route to mesoporous ZnGa<sub>2</sub>O<sub>4</sub> with improved photocatalytic activity in reduction of CO<sub>2</sub><sup>+</sup>," *Angew. Chem.*, vol. 122, no. 36, pp. 6544–6548, Aug. 2010.
- [12] J. B. Varley, J. R. Weber, A. Janotti, and C. G. Van de Walle, "Oxygen vacancies and donor impurities in β-Ga<sub>2</sub>O<sub>3</sub>," *Appl. Phys. Lett.*, vol. 97, no. 14, Oct. 2010, Art. no. 142106.
- [13] D. F. Wang *et al.*, "Low-resistance Ti/Al/Ti/Au multilayer ohmic contact to n-GaN," *J. Appl. Phys.*, vol. 89, no. 11, pp. 6214–6217, Jun. 2001.
- [14] Y. Guo, H. Yan, Q. Song, Y. Chen, and S. Guo, "Electronic structure and magnetic interactions in Zn-doped β-Ga<sub>2</sub>O<sub>3</sub> from first-principles calculations," *Comput. Mater. Sci.*, vol. 87, pp. 198–201, May 2014.
- [15] G. T. Dang, T. Kawaharamura, M. Furuta, and M. W. Allen, "Mist-CVD grown Sn-doped α-Ga<sub>2</sub>O<sub>3</sub> MESFETs," *IEEE Trans. Electron Devices*, vol. 62, no. 11, pp. 3640–3644, Nov. 2015.



**YI-SIANG SHEN** received the B.S. degree in electrical engineering from National Normal University, Kaohsiung, Taiwan, in 2014, and the M.S. degree from the Graduate Institute of Precision Engineering, National Chung Hsing University, Taichung, Taiwan, in 2016. His major research focuses on nitride-based electric power device.



**WEI-KAI WANG** received the B.S. degree in manufacturing engineering from Yuan Ze University, Chungli, Taiwan, in 2000, the M.S. degree in electrical engineering from the University of Chung Hua, Hsinchu, Taiwan, in 2002, and the Ph.D. degree from the Department of Materials Engineering, University of Chung Hsing, Taiwan, in 2006. He is currently an Assistant Professor with the Department of Materials Science and Engineering, Da-Yeh University, Changhua, Taiwan. His research interests include development of GaN-based optoelectronic semiconductors and electric devices.



**RAY-HUA HORNG** (M'07–SM'11–F'02) received the B.S. degree in electrical engineering from National Cheng Kung University, Tainan, Taiwan, in 1987, and the Ph.D. degree in electrical engineering from National Sun Yat-sen University, Kaohsiung, Taiwan, in 1993.

She is currently a Distinguished Professor with the Department of Electronics Engineering, National Chiao Tung University, Hsinchu, Taiwan. Her current research interests include solid-state lighting devices, solar cells, power device, HEMT, flexible electronics, optoelectronics, and nitride and oxide semiconductor MOCVD growths.